



HAL
open science

Transient Vibration Signal Analysis for Bedload Transport Monitoring Systems

Gabriel Vasile, Guy d'Urso, Elena Lungu

► **To cite this version:**

Gabriel Vasile, Guy d'Urso, Elena Lungu. Transient Vibration Signal Analysis for Bedload Transport Monitoring Systems. OCEANS 2017 - OCEANS '17 MTS/IEEE. Our Harsh and Fragile Ocean, Sep 2017, Anchorage, United States. hal-01593491

HAL Id: hal-01593491

<https://hal.science/hal-01593491v1>

Submitted on 26 Sep 2017

HAL is a multi-disciplinary open access archive for the deposit and dissemination of scientific research documents, whether they are published or not. The documents may come from teaching and research institutions in France or abroad, or from public or private research centers.

L'archive ouverte pluridisciplinaire **HAL**, est destinée au dépôt et à la diffusion de documents scientifiques de niveau recherche, publiés ou non, émanant des établissements d'enseignement et de recherche français ou étrangers, des laboratoires publics ou privés.

Transient Vibration Signal Analysis for Bedload Transport Monitoring Systems

Gabriel Vasile

Grenoble-Image-sPeech-Signal-Automatics Lab
CNRS / Univ. Grenoble Alpes
Grenoble Cedex, France, F-38402
gabriel.vasile@gipsa-lab.grenoble-inp.fr

Guy d'Urso

Electricité de France
EDF R&D, STEP
Chatou, France, F-78400
guy.durso@edf.fr

Elena Lungu

SIGNAL INformatics TEChnology
SIGINTEC
Nîmes, France, F-30000
elungu@sigintec.fr

Abstract—This paper proposes a novel framework for detecting and localizing the transients corresponding to the shocks created by sediment impacts on a steel plate. Based on unsupervised hierarchical agglomeration of complex vibration spectra, the derived classification is available for bedload transport monitoring stations in underwater environment.

I. INTRODUCTION

Underwater bedload transport surveys is important for assessing stability issues such as reservoir silting or channel self-cleaning. To this purpose, sediment traps are currently used to derive the sediment balances.

For example, the Birkbeck sampler has become one of the preferred method for in situ bedload measurements. An alternative nonintrusive bedload monitoring instrument is the buried geophone station [1], [2], [3]. Under protection of steel plates, several geophones can provide continuous and automatic measurements, even during large floods. Every stone passing the steel geophone equipped plate generates an impulse recorded by the signal acquisition board. Using a calibrated voltage thresholding scheme the grain impacts are recorded and counted.

In [4], Bogen and Moen used piezoelectric acoustic transducers for bedload monitoring stations in Norway.

Recently, we have proposed, the coupling of ultrasound (US) transducers and with piezoelectric accelerometers for bedload transport monitoring stations. The results obtained in a controlled laboratory environment provided interesting sensitivity capabilities, in accordance with the ground truth. The main objectives of [5] were to increase the operating frequency of the acoustic transducers, to provide consistent calibration and processing and to evaluate the uncertainty of the derived measurements.

To pursue these objectives, an experimental platform, illustrated in Fig. 1-(a) has been developed and tested in the GIPSA-Lab controlled tank system. The following sensors have been employed:

- four ultrasound contact transducers PAC R50 (EM, R2, R3, R4),
- 2 calibrated piezoelectric accelerometers Endevco 233E (A1, A1),
- 1 geophone R.T. Clark (G).

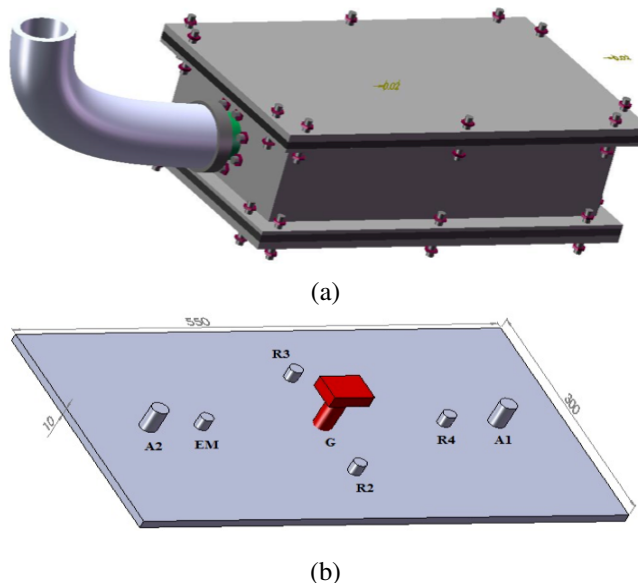


Fig. 1. Multi-sensor bedload transport monitoring platform: (a) general view, (b) setup of the acoustic sensors on the top steel plate.

The EM US transducer has been excited using the ENI 2100L power amplifier and the Picotest G5100A arbitrary signal generator. The received signals from A1, A2, R3, R4 have been conditioned using the Nexus low noise amplifier and recorded using the PXIe-1082 NI system.

This paper proposes a new framework for detecting and localizing the transients (in the passive configuration) corresponding to the shocks created by sediment impacts on the steel plate. The proposed algorithm is based on hierarchical agglomeration of complex vibration spectra. The multivariate segmentation algorithm proposed in [6] is selected: the multimodal signals are analyzed by exploiting the asymptotic distribution of the covariance matrix of the complex spectra.

The paper is structured as follows. Section II illustrates in several steps the general framework of hierarchical agglomeration of complex vibration spectra, while Section III presents both qualitative and quantitative performance assessment. Section IV concludes the paper.

II. HIERARCHICAL AGGLOMERATION OF COMPLEX VIBRATION SPECTRA

The first stage of the proposed segmentation scheme is pre-processing. As each acquisition is triggered on the amplitude level of the sensor exhibiting the fastest response time (the accelerometers in our case), the obtained transient signal is not symmetric. In order to improve the spectral representation, each received signal is circularly shifted to the right and filtered in the common bandwidth. The complex spectrum is obtained by applying the Fast Fourier Transform (FFT) on each signal. One advantage of this representation resides in the fact that it is independent of the time of arrival of each transient.

A. SIRV spectral estimation

In the next step, a multivariate random vector is obtained by concatenating all the complex spectra of the available signals. For each sensor, let \mathbf{k} be the $m \times 1$ complex target vector corresponding to the same frequency range. One way to model the statistical properties of this multivariate random vector leads to Spherically Invariant Random Vectors (SIRV) [7]. It is defined as the product of a square root of a positive random variable τ (variations in power) with an independent circular complex Gaussian vector \mathbf{z} with zero mean and covariance matrix $[M] = E\{\mathbf{z}\mathbf{z}^H\}$ (Gaussian kernel):

$$\mathbf{k} = \sqrt{\tau} \mathbf{z}, \quad (1)$$

where the superscript H denotes the complex conjugate transposition and $E\{\cdot\}$ the mathematical expectation. SIRV representation is not unique, so a normalization condition is necessary. Indeed, if $[M_1]$ and $[M_2]$ are two covariances matrices such that $[M_1] = \alpha[M_2]$. Then $\{\tau_1, [M_1]\}$ and $\{\tau_2 = \tau_1/\alpha, [M_2]\}$ describe the same SIRV. In this paper, the trace of the covariance matrix is normalized to p the dimension of target scattering vector ($p = 3$ for the reciprocal case) [7].

The ML estimator of the normalized covariance matrix under the deterministic texture case is the solution of the following recursive equation :

$$\begin{aligned} [\hat{M}]_{FP} = f([\hat{M}]_{FP}) &= \frac{p}{N} \sum_{i=1}^N \frac{\mathbf{k}_i \mathbf{k}_i^H}{\mathbf{k}_i^H [\hat{M}]_{FP}^{-1} \mathbf{k}_i}, \quad (2) \\ \text{with } Tr([\hat{M}]_{FP}) &= p. \end{aligned}$$

Its asymptotic distribution can be assimilated to the Wishart Probability Density Function (PDF) [7].

In this way, each random vector is described by its normalized covariance matrix, which is independent on the total power at the reception. This will form the feature space for the transient segmentation algorithm.

B. Hierarchical segmentation

The hierarchical segmentation algorithm from [6] is adapted to the vector of complex spectra. The segmentation algorithm is a classical iterative merge algorithm. At each iteration, the two segments which minimize the Stepwise Criterion (SC) are

merged. The basic principle of the hierarchical segmentation algorithm can be divided into three steps :

- 1) Definition of an initial partition (which is formed by the acquired buffers, in our case).
- 2) For each segments pair, SC is computed. Then, the two segments which minimize the criterion are found and merged.
- 3) Stop if the maximum number of merges is reached, otherwise go to step 2.

C. Similarity measure

At each iteration, merging two segments yields a decrease in the log-likelihood function. The stepwise criterion is based on this consideration. The hierarchical segmentation algorithm merges the two segments S_i and S_j which minimizes the loss of likelihood of the partition (which is defined as the sum of likelihoods of partition's segments). The stepwise criterion ($SC_{i,j}$) can be expressed as:

$$SC_{i,j} = MLL(S_i) + MLL(S_j) - MLL(S_i \cup S_j), \quad (3)$$

where $MLL(\cdot)$ denotes the segment maximum log-likelihood function. It is the log-likelihood of the segment (samples in each segment are considered independent realizations) with respect to the assumed probability density function (the Wishart distribution in our case) whose parameters are estimated in the maximum likelihood (hence, the name) sense. Its expression is given by:

$$MLL(S) = \sum_{i \in S} \ln(p_{\mathbf{k}}(\mathbf{k}_i | \theta_S)), \quad (4)$$

θ_S represents the set of distribution parameters (normalized covariance matrix in our case).

1) *Generalized Maximum Log-Likelihood (GMLL)*: In general, the normalized covariance matrix is unknown. One solution consists in replacing the SIRV parameters by their estimates. After replacing the covariance matrix $[M]$ by its respective ML estimators, the stepwise criterion becomes:

$$SC_{i,j} = GMLL(S_i) + GMLL(S_j) - GMLL(S_i \cup S_j), \quad (5)$$

where $GMLL(S)$ is the generalized maximum log-likelihood function for segment S .

2) *For the Wishart PDF*: the generalized maximum log-likelihood function for segment S is:

$$GMLL(S) = -pN \ln(\pi) - N \ln \left\{ |[\hat{M}_{ML}]| \right\} \quad (6)$$

where $[\hat{M}_{ML}]$ is the ML estimator of $[M_{ML}]$ for segment S (2).

D. Stop criterium

The use of the L-method [8] has been considered in this paper. This method employs the very error (quality) function that is used to perform cluster merging during the hierarchical segmentation algorithm, specifically the Log-Likelihood Function (LLF) of the partition (i.e. the sum of the MLL values for all the segments of the partition). As this is readily computed

during the proposed method, no further computational effort is required. The *knee* of this error function is identified and the optimal number of clusters is chosen at that point. The *knee* of a curve is somewhat similar to the point of maximum curvature.

III. RESULTS AND DISCUSSION

The proposed experimentations were carried in the GIPSA-Lab controlled tank system. Figs. 2 and 3 illustrate the transient signals obtained from the four sensors (accelerometers and ultrasound) in passive configuration, after right circular shift and common band pass filtering.

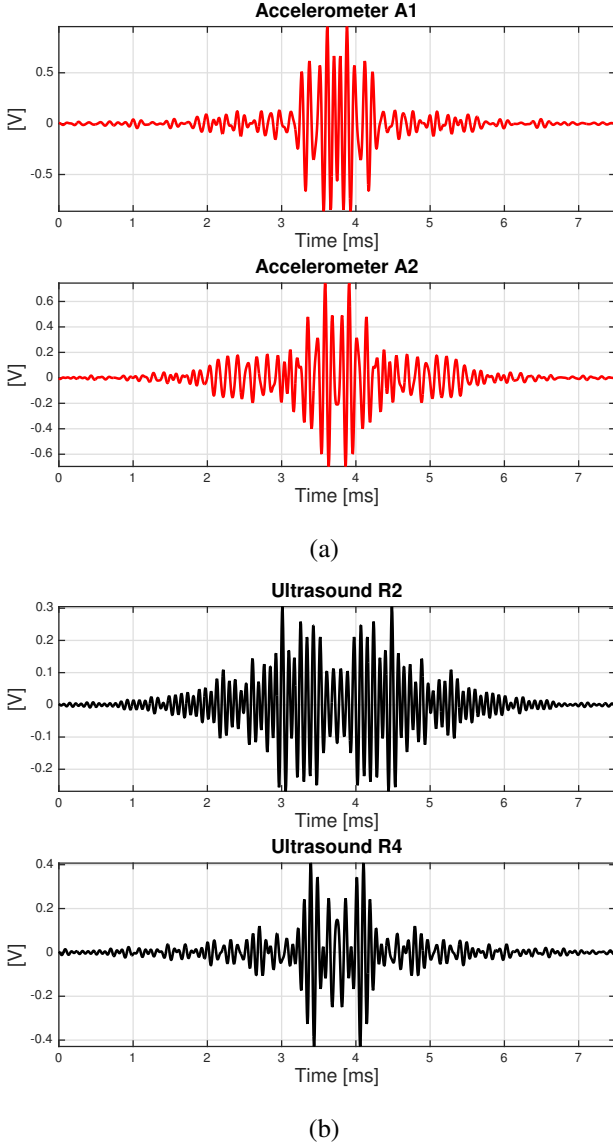


Fig. 2. Sensors recordings in passive configuration, 1 buffer triggered by A1: (a) accelerometers and (b) ultrasound transducers.

In order to build the data base, five metallic balls with different diameters have been selected for the experiments. For each ball, 25 independent impacts have been recorded using the bedload transport monitoring platform from Fig. 1.

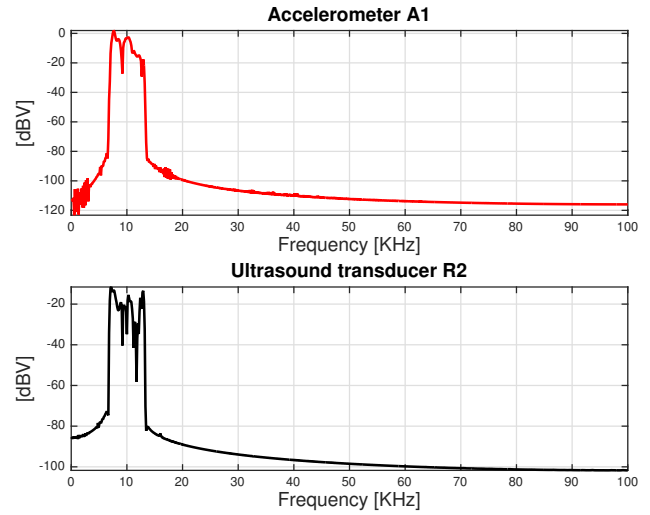


Fig. 3. Sensors recordings spectra in passive configuration, 1 buffer triggered by A1: accelerometer A1 (up) and ultrasound transducer R2 (down).

The balls have been manually released from the surface of the water at approximately the same position on the metallic plate. An independent buffer has been recorded for each impact with the four sensors simultaneously and coherently.

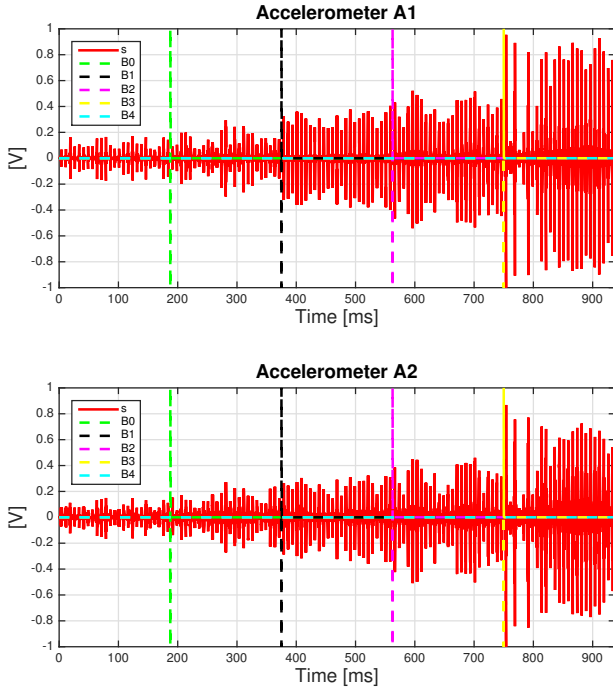
After concatenating the 25×5 buffers, Fig. 4 shows the derived signals used to test the proposed hierarchical agglomeration algorithm.

The obtained results are presented in the confusion matrix from Tab. I. There are at least two facts to be noticed. Firstly, the diagonal structure of the confusion matrix reveals a rather good classification accuracy. Secondly, the L-method stopped the segment merging at 8 classes. This is explained by the fact that the impacts of the ball B4 have been splitted in two classes, while some impacts from B1 and B3 generated two additional classes. This is in agreement with the subjective visual assessment of the signals from Fig. 4.

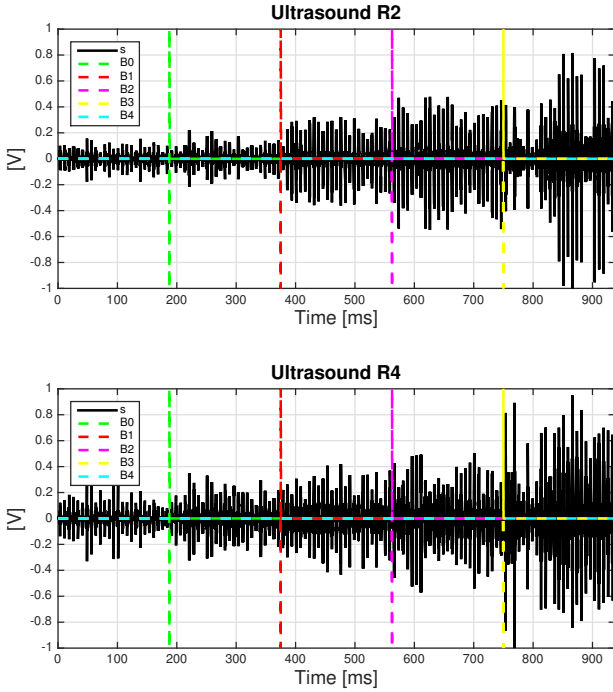
TABLE I
QUANTITATIVE PERFORMANCE ASSESSMENT: CONFUSION MATRIX. SC (FROM 1 TO 8) ARE THE CLASSES OBTAINED BY THE PROPOSED ALGORITHM, WHILE TC (FROM 1 TO 5) ARE THE GROUND TRUTH BASED CLASSES.

| | TC 1 | TC 2 | TC 3 | TC 4 | TC 5 |
|------|------|------|------|------|------|
| SC 1 | 25 | 8 | 0 | 0 | 0 |
| SC 2 | 0 | 15 | 6 | 0 | 0 |
| SC 3 | 0 | 0 | 19 | 8 | 0 |
| SC 4 | 0 | 0 | 3 | 13 | 5 |
| SC 5 | 0 | 0 | 0 | 0 | 11 |
| SC 6 | 0 | 0 | 0 | 0 | 9 |
| SC 7 | 0 | 0 | 0 | 4 | 0 |
| SC 8 | 0 | 2 | 0 | 0 | 0 |

Finally, an overall quantitative indicator of the performance of the proposed algorithm is the classification accuracy A ,



(a)



(b)

Fig. 4. Sensors recordings in passive configuration, 1 buffer triggered by A1: (a) accelerometers and (b) ultrasound transducers.

defined as:

$$A = \frac{\sum_{i=0}^5 TP_{Bi} + \sum_{i=0}^5 TN_{Bi}}{5T} \times 100, \quad (7)$$

with TP_{Bi} the true positive for the metallic ball Bi , TN_{Bi} the true negative and $T = 125$ the total population. After fusing the classes SC 5 and SC 6, SC 2 and SC 8, SC 4 and SC 7, we can compute the total classification accuracy according to Eq. 7.

The obtained value is $A = 90.9\%$.

IV. CONCLUSION

This paper proposed a new framework for detecting and localizing the transients corresponding to the shocks created by sediment impacts on the steel plate. The proposed classification strategy is based on hierarchical agglomeration of complex vibration spectra: the multimodal signals were analyzed by exploiting the asymptotic distribution (SIRV) of the normalized covariance matrix. Qualitative and quantitative performance assessment has been carried out using vibration signals recorded by the multi-sensor bedload transport monitoring platform from the GIPSA-Lab.

Future work will enroll in two main directions. Firstly, we will try to explore as much as possible all the benefits of the proposed classification algorithm in real life scenarios. Secondly, we will continue with improving the description of transient vibration signals by using non-stationary time-frequency representations instead of the Fourier transform.

REFERENCES

- [1] D. Rickenmann, J. M. Turowski, B. Fritschi, A. Klaiber, and A. Ludwig, "Bedload transport measurements at the Erlenbach stream with geophones and automated basket samplers," *Earth Surface Processes and Landforms*, vol. 37, no. 9, pp. 1000–1011, 2012.
- [2] D. Rickenmann, J. M. Turowski, B. Fritschi, C. Wyss, J. B. Laronne, R. Barzilai, I. Reid, A. Kreisler, J. Aigner, H. Seitz, and H. Habersack, "Bedload transport measurements with impact plate geophones: comparison of sensor calibration in different gravel-bed streams," *Earth Surface Processes and Landforms*, vol. 39, no. 7, pp. 928–942, 2014.
- [3] R. Hilldale, W. Carpenter, B. Goodwiller, J. Chambers, and T. Randle, "Installation of impact plates to continuously measure bed load: Elwha river, Washington, USA," *J. Hydraul. Eng.*, vol. 141, no. 3, pp. 06014023, 2015.
- [4] J. Bogen and K. Moen, "Bedload measurements with a new passive acoustic sensor," in *Erosion and Sediment Transport Measurement in Rivers: Technological and Methodological Advances*, 2003, pp. 181–192.
- [5] G. Vasile, G. d'Urso, R. Charlatchka, and E. Lungu, "Calibration of an active ultrasound bedload monitoring system for underwater environments," in *Proceedings of the MTS/IEEE North American OCEANS conference, Washington, DC, USA*, 2015, pp. 1–4.
- [6] L. Bombrun, G. Vasile, M. Gay, and F.C. Totir, "Hierarchical segmentation of polarimetric SAR images using heterogeneous clutter models," *IEEE Transactions on Geoscience and Remote Sensing*, vol. 2, no. 46, pp. 726–737, 2011.
- [7] G. Vasile, F. Pascal, J.P. Ovarlez, P. Formont, and M. Gay, "Optimal parameter estimation in heterogeneous clutter for high-resolution polarimetric SAR data," *IEEE Geoscience and Remote Sensing Letters*, vol. 8, no. 6, pp. 1046–1050, 2011.
- [8] S. Salvador and P. Chan, "Determining the number of clusters/segments in hierarchical clustering/segmentation algorithms," in *16th IEEE International Conference on Tools with Artificial Intelligence, ICTAI 2004*, 2004, pp. 576–584.